Rapid structural alterations of the active zone lead to sustained changes in neurotransmitter release

Jacob Matz[a], Andrew Gilyan[a,b], Annette Kolar[a,b], Terrence McCarvill[a], and Stefan R. Krueger[a,b,1]

[a]Department of Physiology and Biophysics and [b]Neuroscience Institute, Dalhousie University, Halifax, NS, Canada B3H 1X5

Edited by Charles F. Stevens, The Salk Institute for Biological Studies, La Jolla, CA, and approved April 6, 2010 (received for review June 2, 2009)

The likelihood with which an action potential elicits neurotransmitter release, the release probability (p_r), is an important component of synaptic strength. Regulatory mechanisms controlling several steps of synaptic vesicle (SV) exocytosis may affect p_r, yet their relative importance in determining p_r and eliciting temporal changes in neurotransmitter release at individual synapses is largely unknown. We have investigated whether the size of the active zone cytomatrix is a major determinant of p_r and whether changes in its size lead to corresponding alterations in neurotransmitter release. We have used a fluorescent sensor of SV exocytosis, synaptophysin-pHluorin, to measure p_r at individual synapses with high accuracy and employed a fluorescently labeled cytomatrix protein, Bassoon, to quantify the amount of active zone cytomatrix present at these synapses. We find that, for synapses made by a visually identified presynaptic neuron, p_r is indeed strongly correlated with the amount of active zone cytomatrix present at the presynaptic specialization. Intriguingly, active zone cytomatrices are frequently subject to synapse-specific changes in size on a time scale of minutes. These spontaneous alterations in active zone size are associated with corresponding changes in neurotransmitter release. Our results suggest that the size of the active zone cytomatrix has a large influence on the reliability of synaptic transmission. Furthermore, they implicate mechanisms leading to rapid structural alterations at active zones in synapse-specific forms of plasticity.

release probability | synaptic vesicle docking | active zone cytomatrix | plasticity | pHluorin

Synaptic transmission between most neurons is unreliable as a presynaptic action potential elicits neurotransmitter (NT) release at any individual synapse with a release probability (p_r) of less than one. This probability can vary considerably among synapses of the same axon, often in a target-specific manner (1–3). Similarly, synapses onto a single neuron often display widely varying release probabilities (4–7). Moreover, p_r can undergo sustained activity-dependent changes over time (8–11). These observations suggest that p_r is an important determinant of synaptic strength that is tightly controlled by the presynaptic neuron and/or, indirectly, by its postsynaptic target.

Although numerous studies have highlighted specific regulatory mechanisms affecting p_r of synapses at rest, a concise picture of how p_r at individual synapses is determined is only beginning to emerge. Synaptic vesicle (SV) exocytosis is a multistep process during which SVs have to dock at the active zone cytomatrix and undergo a priming step before they are "readily releasable," i.e., immediately available for fusion with the plasma membrane in response to calcium influx through voltage-gated calcium channels (12). Evidence that the size of a synapse's readily releasable pool (RRP) of SVs is closely correlated with its p_r (7, 13) suggests that p_r is mainly determined by processes upstream of calcium entry and calcium-induced SV fusion. Among these processes, mechanisms affecting the rate of priming or the relative fusion competence of primed SVs may crucially regulate the size of the RRP, as studies of proteins implicated in SNARE complex formation suggest (14, 15). On the other hand, mechanisms regulating SV docking may decisively determine RRP size and p_r, a notion supported by ultrastructural evidence that the size of the RRP at a synapse is closely correlated with the number of SVs docked at its active zone (16). Interestingly, the number of docked SVs is known to correlate well with active zone size (17, 18), indicating that, by limiting the number of docked SVs, the size of its active zone may be a major determinant of RRP size.

Taken together, this chain of evidence—a strong correlation between active zone size and the number of docked SVs (17, 18), similarity of the number of docked SVs and RRP size (16), and a strong correlation between RRP size and p_r (7, 13)—suggests that p_r may be controlled by active zone size. However, this hypothesis has not been verified directly, in part due to technical challenges in quantifying the p_r of individual synapses with high accuracy. Moreover, although active zone size has been shown to change homeostatically in response to disuse in a slow and global manner (13), it remains unclear whether fast, synapse-specific structural changes of active zones occur that lead to sustained alterations in NT release. In this study, we address these questions by using a genetically encoded fluorescent sensor of SV exocytosis, synaptophysin-pHluorin, to quantify p_r and a fluorescently labeled active zone protein, tdTomato-Bassoon, to obtain a measure of active zone size and plasticity at individual synapses between hippocampal neurons in dissociated cultures.

Results

The release probability of individual synapses can be accurately determined using sypH2 as a genetically encoded sensor of SV exocytosis. Sensors containing superecliptic pHluorin (19, 20) fused to a SV protein are increasingly used to study SV cycling. Previous studies have demonstrated that the sensitivity of these sensors can be high enough to allow the detection of exo- and endocytosis of individual SVs (21–23). This led us to investigate whether a SV exocytosis sensor with particularly high signal-to-noise ratio, synaptophysin-pHluorin 2× (sypH2) is suitable to determine p_r of individual synapses. In hippocampal neurons transfected with sypH2, fluorescence was concentrated at axonal varicosities and increased upon delivery of short stimulus trains (Fig. 1*A*). At these varicosities, isolated stimuli frequently elicited fluorescence increases that were likely due to fusion of single SVs with the plasma membrane but barely distinguishable from noise (Fig. 1*B*). To determine p_r, i.e., the likelihood of SV fusion at a release site in response to a stimulus, we took two different approaches. First, averaging of fluorescence traces in response to 100 stimuli delivered at low frequency (0.2 Hz) yielded an average fluorescence response of each synapse to a single stimulus (Fig. 1 *A* and *C*), whose amplitude is a relative measure of p_r at that synapse. In a second approach, we determined for each stimulus trial

Author contributions: S.R.K. designed research; J.M., A.G., A.K., T.M., and S.R.K. performed research; J.M., A.K., and S.R.K. analyzed data; and S.R.K. wrote the paper.

The authors declare no conflict of interest.

This article is a PNAS Direct Submission.

[1]To whom correspondence should be addressed. E-mail: stefan.krueger@dal.ca.

This article contains supporting information online at www.pnas.org/lookup/suppl/doi:10.1073/pnas.0906087107/-/DCSupplemental.

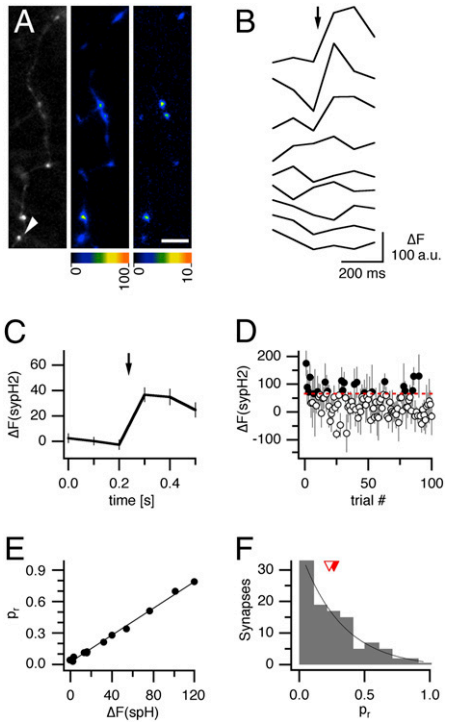

Fig. 1. SypH2 allows a quantification of p_r at individual synapses. (*A*) Baseline sypH2 fluorescence of a transfected neuron (*Left*), sypH2 fluorescence changes in response to a train of 40 stimuli at 20 Hz (average of response to 10 consecutive trains; *Center*), and fluoresence changes in response to isolated stimuli at low frequency (average of responses to 100 stimuli delivered at 0.2 Hz; *Right*). Fluorescence increases are presented as false color images. (Scale bar, 5 μm.) (*B*) Fluorescence changes at a single synapse, indicated with an arrowhead in *A* in response to isolated stimuli at 0.2 Hz. (*C*) Average of sypH2 fluorescence change at the same synapse in response to 100 stimuli. The amplitude of the averaged response is an indirect measure of p_r at that synapse. (*D*) Time-averaged changes in sypH2 fluorescence at the same synapse were calculated for each stimulation trial. Error bars denote SE. If fluorescence changes calculated exceeded a noise-based threshold (*Materials and Methods*), the stimulation was considered to have elicited neurotransmitter release (black circles), otherwise, it was counted as failure (white circles). P_r was calculated as $p_r = S/(S + F)$, where S is the number of trials resulting in neurotransmitter release and F the number of trials that did not. (*E*) Correlation of amplitudes of averaged sypH2 responses and release probabilities, calculated as shown in D, for the 11 synapses identified in this experiment ($r = 0.996$). (*F*) Distribution of release probabilities of 106 synapses from five experiments. Median (white arrowhead) and mean (red arrowhead) as well as an exponential fit of the distribution are shown.

whether a stimulus resulted in SV exocytosis by time-averaging the fluorescence in time lapse frames over 300 ms before the stimulus and subtracting this averaged baseline fluorescence from an average of time-lapse frames obtained over 300 ms after the stimulus. A stimulus was considered to have resulted in SV exocytosis if the time-averaged increase in fluorescence exceeded a threshold determined by the noise of the optical recording (see *Materials and Methods* for details; Fig. 1*D*). In all experiments performed, the absolute values of p_r obtained with this approach correlated extremely well with the amplitude of the averaged fluorescence response (range of Pearson product-moment correlations $0.980 \leq r \leq 0.996$ in five experiments in which all synapses were made by a single presynaptic neuron; Fig. 1*E*), suggesting that both methods provide very reliable measures of p_r. As a final assessment of our technique, we determined the frequency of occurrence of p_r values at 106 synapses in five experiments. The p_r distribution (Fig. 1*F*) was broad and skewed toward small values with a mean of 0.27, in agreement with previously obtained estimates of p_r at synapses between hippocampal neurons (6, 24, 25). Together, these results demonstrate that p_r at individual synapses can be quantified using sypH2 as a genetically encoded sensor of SV exocytosis.

The size of the active zone cytomatrix is a major determinant of RRP and p_r. The transfection of sypH2 into cultures of hippocampal neurons yielded expression in a small subset of neurons, allowing us to compare NT release at multiple active zones in single, optically identified axons. Thus, we were able to investigate determinants of RRP and p_r at release sites of an individual neuron, in isolation from factors that create additional variation between neurons. Specifically, we were interested in whether the size of active zones, reported to vary greatly between excitatory hippocampal synapses (17), crucially determines their p_r. The size of active zones is close to the diffraction-limited resolution of light microscopy, and cannot be accurately measured in our experiments. It is possible, however, to quantify the amount of active zone cytomatrix at a synapse using a fluorescently tagged active zone cytomatrix protein, provided that this protein is distributed in a homogeneous manner in all active zone cytomatrices of a transfected presynaptic neuron. We found that Bassoon, previously shown to be highly localized to active zone cytomatrices (26), is ideally suited for this purpose. The fluorescence of tdTomato-tagged Bassoon (tdT-Bsn) at synaptic sites correlated well with the amount of other active zone cytomatrix proteins such as Piccolo and RIM (Fig. S1), demonstrating its homogeneous distribution within active zones. Thus, differences in tdT-Bsn fluorescence intensity between active zones of a transfected neuron faithfully reflect differences in the amount of active zone cytomatrix present at the synapse. Under the assumption that active zone cytomatrices have similar densities, tdT-Bsn fluorescence is also an indirect measure of active zone size.

In cotransfected neurons, tdT-Bsn labeled active zones colocalized extremely well with sites of stimulation-evoked sypH2 increases (Fig. 2*A*). To assess the size of the pool of docked and primed SVs (RRP) at tdT-Bsn positive release sites, we elicited SV exocytosis with short stimulus trains, 40 stimuli at 20 Hz (13). The p_r at each release site was assessed using isolated stimuli at low frequency (0.2 Hz). As shown in Fig. 2, release sites with strong tdT-Bsn fluorescence tended to display strong increases in sypH2 fluorescence in response to stimulus trains (Fig. 2 *A* and *B*) and to isolated stimuli at low frequency (Fig. 2 *A* and *C*), suggesting that synapses with large active zone cytomatrices also had large releasable pools of SVs and release probabilities. An analysis of all release sites in the experiment shown in Fig. 2 and in four other experiments revealed that the sypH2 fluorescence increases in response to stimulus trains (Fig. 2*D*) and isolated stimuli at low frequency (Fig. 2*E*) correlated very well with the tdT-Bsn fluorescence intensity at each release site. Overall, we found median correlation coefficients between measures of active zone cytomatrix size and RRP or p_r, respectively, of $r = 0.948$ (range: 0.889–0.966) and $r = 0.880$ (range: 0.833–0.953). A change in the extracellular calcium concentration from 2 to 4 mM led to a significant increase in the slope of the correlation between tdT-Bsn fluorescence and average sypH2 responses to isolated stimulation but no substantial changes in the quality of the correlation (Fig. S2). The tight correlation between amount of active zone cytomatrix, RRP size, and p_r is further illustrated by the distribution of the residuals of these fits for 106 release sites in five experiments at an extracellular calcium concentration of 2 mM (Fig. 2 *F* and *G*). For 77.4% of all release sites, the experimentally determined number of docked and primed SVs deviated by not more than one from the value expected from its tdT-Bsn fluorescence (Fig. 2*F*). Similarly, for 73.6% of release sites, p_r fell within 0.1 of the expected value (Fig. 2*G*). These data demonstrate that RRP size and p_r at

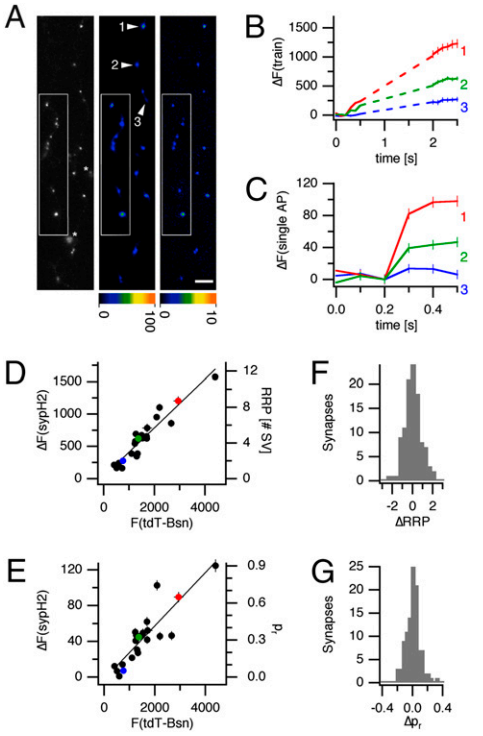

Fig. 2. RRP size and p_r at hippocampal synapses strongly correlate with active zone size. (*A*) tdT-Bsn fluorescence (*Left*) and sypH2 fluorescence changes in response to stimulus trains of 40 stimuli at 20 Hz (*Center*) and isolated stimuli at 0.2 Hz (average of 100 trials, *Right*) in a tdT-Bsn and sypH2-transfected neuron. (*Inset*) Additional synapses located on another axonal branch. (Scale bar, 5 μm.) (*B*) SypH2 fluorescence increase in response to the stimulus trains at three synapses (arrowheads in *A*). (*C*) Averaged responses to isolated stimuli at low frequency at the same synapses. (*D*) Correlation between sypH2 responses to the stimulus trains and tdT-Bsn fluorescence for 22 synapses in this experiment (r = 0.948). (*E*) Correlation between average sypH2 responses to isolated stimuli and tdT-Bsn fluorescence (r = 0.902). Release probabilities for each synapse (right axis) were obtained through linear regression of p_r measures obtained by trace averaging and time averaging as shown in Fig. 1*E*. This method also allowed calculation of the average sypH2 fluorescence per exocytosed SV (in this experiment, F_{SV} = 138.2), enabling us to estimate RRP sizes (right axis in *D*). (*F*) Residuals of linear regressions between sypH2 increases in response to stimulus trains (RRP size) and tdT-Bsn fluorescence at 106 synapses in five experiments. (*G*) Residuals of linear regressions between average sypH2 increases in response to isolated stimuli (p_r) and tdT-Bsn fluorescence at the same synapses.

hippocampal synapses correlate very strongly with the amount of active zone cytomatrix present at the presynaptic specialization.

Active zones are subject to synapse-specific changes in size on a time scale of minutes. Considering the tight correlation between active zone cytomatrix size and measures of neurotransmitter release, it is conceivable that structural alterations at presynaptic specializations could contribute to changes in RRP size and p_r. Previous studies have suggested that active zones of hippocampal synapses can change in size in a homeostatic manner over days in response to global alterations in neuronal activity (13), possibly due to altered turnover of active zone cytomatrix components. It has not been investigated, however, whether active zone cytomatrices can also undergo structural changes in a more synapse-specific manner on a faster time scale. We addressed this possibility by using tdT-Bsn to detect structural alterations of synaptic active zone cytomatrices that might occur at synapses between hippocampal neurons. For this purpose, we used cultures 14–21 days after plating, i.e., well after the onset of synapse formation and spinogenesis. To distinguish synaptic active zones from release sites without postsynaptic apposition, which comprise up to a third of all release sites formed by hippocampal neurons in culture (27), and to limit our analysis to axospinous synapses, which constitute the majority of glutamatergic synapses between hippocampal neurons, we subsequently transfected hippocampal neurons with tdT-Bsn and YFP-labeled actin. In time-lapse imaging experiments, we then analyzed structural changes of active zones at axospinous synapses between tdT-Bsn expressing presynaptic neurons and postsynaptic neurons in which spines were labeled with YFP-actin. Although tdT-Bsn fluorescence remained relatively unchanged at the majority of synapses, it changed dramatically at others, often on a time scale of minutes, due to recruitment of active zone cytomatrix clusters from adjacent axonal regions or mobilization of the cytomatrix material from the synaptic site (Fig. 3 *A* and *B* and Movie S1). A quantification of tdT-Bsn fluorescence changes at 158 axospinous synapses from experiments in three cultures revealed that during 30-min time-lapse experiments, active zone sizes increased or decreased by more than half at 18.3% of all synapses analyzed (Fig. 3*C*). Although comparatively large changes were more frequent at synapses with small active zones, even large synapses underwent significant changes in active zone size (Fig. 3*D*). These observations reveal that presynaptic specializations are subject to structural plasticity leading to synapse-specific changes in active zone size on a time scale of minutes.

Changes in active zone size are associated with changes in RRP and p_r. To address whether these rapid changes in active zone size at individual synapses lead to alterations in NT release, we again cotransfected cultures of hippocampal neurons with sypH2 and tdT-Bsn. Following an initial quantification of sypH2 fluorescence increases in response to isolated and train stimulation, as well as tdT-Bsn fluorescence, we incubated the culture for another 5–6 h and then reassessed measures of p_r, RRP and active zone cytomatrix size. After this second quantification, we identified axospinous synapses of transfected neurons by staining with

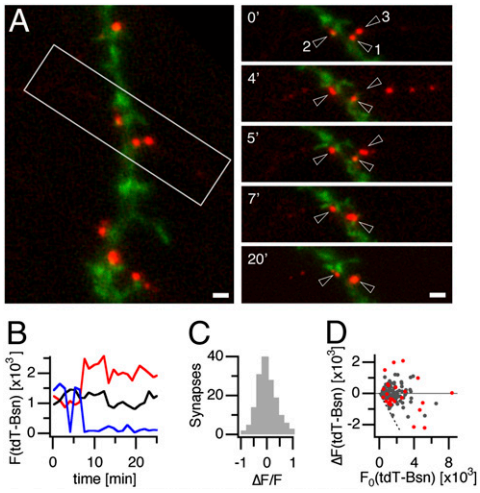

Fig. 3. Structural plasticity of active zones. (*A Left*) Image of a synaptically connected pair of hippocampal neurons. The presynaptic neuron expresses tdT-Bsn (red), the postsynaptic neuron Venus actin (green). (*Right*) Consecutive images of the boxed region. Time stamps indicate time elapsed in minutes. (Scale bar, 2 μm.) (*B*) tdT-Bsn fluorescence at active zones of the synapses labeled in *A*. (*C*) Distribution of fluorescence changes at 158 axospinous synapses over 30 min. Data were collected in five experiments using three different cultures. (*D*) tdT-Bsn fluorescence changes as a function of initial tdT-Bsn fluorescence from the same data set. Red dots represent synapses of a single time-lapse experiment. The dotted line indicates complete loss of tdT-Bsn fluorescence at an axospinous apposition.

fluorescently labeled phalloidin and MAP2-antibodies to visualize actin-rich spines and dendritic tubulin. Again, tdT-Bsn fluorescence was found to change significantly at a subset of axospinous synapses (Fig. 4*A* and Fig. S3*A*), indicating alterations of active zone size. These changes were often paralleled by significant changes in sypH2 responses to stimulus trains and isolated stimuli, suggesting concomitant alterations in RRP size and p_r (Fig. 4 *A–C* and Fig. S3 *B–C*). To address if alterations in active zone size correlate with alterations in NT release, we plotted changes in the syph2 fluorescence response to the stimulus train (Fig. 4*D*) and isolated stimuli at low frequency (Fig. 4*E*) against changes in tdT-Bsn fluorescence observed for each of the 45 synapses in this experiment. The measure for changes in RRP size correlated highly ($r = 0.697$), that for p_r moderately ($r = 0.544$) with alterations in tdT-Bsn fluorescence over the time period. In two other experiments executed in the same manner, similar correlations between tdT-Bsn fluorescence and RRP size (range 0.697–0.777), as well as p_r (range 0.544–0.601), were observed. To collectively evaluate data from all three experiments, we binned a total of 122 synapses for changes in RRP size or p_r and plotted average changes in tdT-Bsn fluorescence for these bins (Fig. 4 *F* and *G*). The significant correlations between the tdT-Bsn fluorescence and RRP size, as well as p_r, strongly suggest that synapse-specific changes in active zone size contribute to changes in NT release at these synapses. It should be noted that, although we chose to assess changes in NT release over a 5- to 6-h period, alterations in RRP and p_r paralleling changes in active zone cytomatrix size were observed at some synapses over much shorter time spans (Fig. S4), confirming that structural alterations of active zone cytomatrices and concomitant changes in NT release occur rapidly.

Discussion

The findings of this study suggest that the size of the active zone cytomatrix may be a major determinant of RRP size and p_r at synapses between hippocampal neurons. Moreover, they demonstrate that active zones are subject to frequent synapse-specific structural alterations, which in turn lead to corresponding changes in NT release.

Evidence for a central role of active zone size in the determination of RRP size and p_r comes from our finding that SV exocytosis in response to short high-frequency stimulus trains or isolated stimuli at low frequency is highly correlated with the amounts of a fluorescently labeled active zone cytomatrix protein, tdT-Bsn. Active zone cytomatrices are highly ordered subcellular structures (28, 29) whose assembly involves the recruitment of equivalent amounts of Bassoon and other active zone cytomatrix proteins (30). tdT-Bsn is homogeneously distributed within active

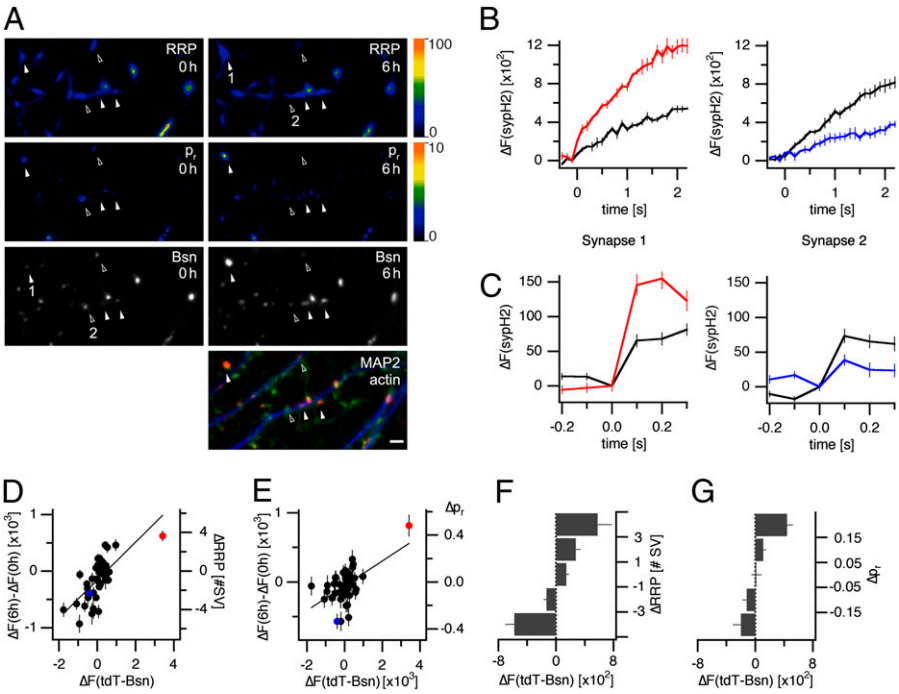

Fig. 4. Changes in active zone size lead to corresponding alterations in RRP size and p_r. Neurons transfected with sypH2 and tdT-Bsn were used in a time lapse experiment to identify synapses at which p_r, RRP, and/or active zone cytomatrix sizes changed over the course of 6 h. Cells were then fixed and stained with anti-MAP2 antibodies and Cy5-conjugated phalloidin to visualize dendritic tubulin (blue) and actin (green), respectively, allowing the identification of axodendritic synapses. Only active zone cytomatrices within 1 μm of a MAP2-positive dendritic shaft that were colocalized with a phalloidin-visualized spine were included in the subsequent analysis. (*A*) Responses to train stimulation (RRP) and average responses to isolated stimuli at 0.2 Hz (p_r) and tdT-Bassoon fluorescence (Bsn) at several synapses at the beginning of the experiment (*Left*) and after 6 h (*Right*). Filled or open arrowheads denote synapses at which tdT-Bsn fluorescence as well as RRP and p_r measures increase or decrease, respectively. (*Bottom Right*) The same field after visualization of actin and MAP2 (MAP2/actin). (Scale bar, 4 μm.) (*B*) At the synapses denoted with 1 and 2 in (*A*), sypH2 responses stimulus trains increased or decreased significantly ($P < 0.001$) in parallel with changes in tdT-Bsn fluorescence ($P < 10^{-4}$ and $P < 0.01$, E). (*C*) At the same synapses, a significant enhancement or attenuation, respectively, in the averaged response to isolated stimuli at 0.2 Hz was observed ($P < 0.001$). (*D*) Correlation between changes in the sypH2 response to stimulus trains delivered at the onset of the experiment (ΔF_1) and after 6 h (ΔF_2), and changes in tdT-Bsn fluorescence for 45 synapses in this experiment ($r = 0.697$, $P < 10^{-6}$, Pearson product moment correlation). Synapses 1 and 2 are highlighted in red and blue, respectively. (*E*) Correlation between changes in the average sypH2 response to isolated stimuli delivered at the onset (ΔF_1) and end of the experiment (ΔF_2), respectively, and changes in tdT-Bsn fluorescence ($r = 0.544$, $P < 0.001$). sypH2 fluorescence changes were converted into estimates of changes in RRP or p_r as outlined in the legend to Fig. 2. (*F*) Changes in tdT-Bassoon fluorescence that occurred at a total of 122 synapses in three experiments that were binned according to the change in RRP size occurring during a 5- to 6-h experiment. (*G*) Changes in tdT-Bassoon fluorescence at the same 122 synapses, binned for changes in p_r.

zone cytomatrices (Fig. S1) and faithfully reflects the amount of active zone cytomatrix present at a synapse. The simplest model consistent with our finding that RRP size and p_r at a synapse correlate highly with the amount of active zone cytomatrix present is that the size of the active zone, by limiting the number of docked synaptic vesicles, crucially determines these parameters of NT release. Based on our data alone, however, we cannot rule out the alternative interpretation that other components associated with active zone cytomatrices, such as synaptic vesicle pools that may be coregulated with active zone size, scale RRP and/or p_r independently.

The very high correlations between measures of RRP size, p_r, and active zone size obtained in this study are somewhat surprising given previous reports of positive, yet somewhat lower, correlations between the number of docked SVs at an active zone and RRP size (16) and between RRP size and p_r (13), which would indicate a smaller influence of active zone size on NT release. This apparent discrepancy may be explained by two consequences of our experimental approach. First, the expression of a genetically encoded sensor of SV exocytosis in a small subset of neurons allowed us to compare different presynaptic specializations of individual, optically identified presynaptic neurons. In contrast, prior studies generally involved loading of styryl dyes into SVs at all release-competent presynaptic specializations to measure NT release, leading to comparison of NT release sites from different presynaptic neurons. The differential expression or regulation of components of the priming machinery and voltage-gated calcium channels in different neurons differentially affects NT release, thus obscuring the dominating influence active zone size may have in the control of RRP size and p_r in individual presynaptic neurons. As a second consequence of our experimental approach, the use of sypH2 allowed us to take repeated measures of responses to stimulus trains and a larger number of isolated stimuli at low frequency to quantify RRP size and p_r, respectively. Thus, our measurements are likely less sensitive to the large trial-to-trial variability inherent in NT release measurements than are methods relying on the use of styryl dyes, for which increasing background staining with continued application typically limits repeated quantifications. Taken together, these consequences of our experimental approach likely accounted for the higher correlations between active zone size and NT release.

It should be noted that our finding of a high correlation between active zone size and RRP size does not challenge the importance of mechanisms affecting SV priming in the regulation of the readily releasable pool of SVs (14, 15). In our study, RRP size varied to a small but significant extent from the value expected from their active zone size at a subset of synapses, allowing for the possibility that differences in the rate of SNARE complex formation or in the fusion competence of primed SVs affect RRP sizes in a synapse-specific manner. Moreover, the regulation of priming may affect NT release in a global way, scaling RRP sizes and p_r at all active zones in a given presynaptic neuron. Our findings do indicate, however, that in the majority of hippocampal neurons, sustained synapse-specific alterations of p_r and especially RRP size are likely to be limited in magnitude in the absence of changes in active zone size.

Given the many reports of considerable plasticity of NT release at hippocampal synapses (8–11, 31, 32), the finding that RRP size and p_r are highly correlated with active zone size raises the question of whether structural alterations at presynaptic specializations contribute to sustained changes in NT release. In this study, we show that active zones of axospinous synapses between hippocampal neurons in culture are subject to frequent changes in size. These alterations in active zone size occur on a time scale of minutes, resulting from recruitment and mobilization of active zone cytomatrix material to and from the synapse. At first sight, our observation is in apparent contradiction to an earlier report of a slow turnover of Bassoon at active zone cytomatrices (33), determined using fluorescence recovery after photobleaching (FRAP) and photoactivation techniques. However, this study also showed significant heterogeneity in FRAP recovery of EGFP-Bassoon between individual synapses and noted the exchange of Bassoon between synapses on a faster timescale. Taken together, our data and the results from Tsuriel et al. (33) suggest that, although the turnover of Bassoon by protein synthesis and degradation mechanisms may be relatively slow, local redistribution of active zone cytomatrix components leads to rapid changes in the size of active zone cytomatrices at a subset of synapses. We demonstrate in this study that these alterations of cytomatrix size lead to concomitant changes in RRP size and p_r. Interestingly, correlations between alterations in active zone size and changes in RRP size were high, whereas those between active zone size alterations and p_r changes were more moderate. This finding indicates that changes in active zone size play a predominant role in the alteration of RRP size, whereas additional mechanisms likely contribute to sustained changes in p_r.

It is important to point out that although structural changes of active zones are common in cultures of dissociated hippocampal neurons and represent an important mechanism for sustained changes in NT release in this preparation, they may not necessarily be frequent occurrences at cortical synapses in vivo. Fluorescently labeled active zone proteins such as tdT-Bsn, which can detect structural changes at active zones with high sensitivity, have not, to our knowledge, been used in vivo. However, studies using cytoplasmic and membrane-bound EGFP as volume markers to investigate changes of axonal structures in the intact mammalian cortex provide some interesting clues (34, 35). These studies investigated the structural plasticity of axonal varicosities in the adult somatosensory and visual cortex, respectively, and reported that a large fraction of presynaptic specializations, 15–60% depending on the type of afferents, appears and disappears over the time course of a month (34). These findings suggest that presynaptic specializations in the intact mammalian cortex are subject to substantial structural plasticity and give a first indication that structural alterations of release sites similar to those described in this study may also occur in vivo. However, further studies in more intact preparations are needed to directly address the existence and prevalence of changes in active zone size, which clearly could represent an important mechanism in the synapse-specific regulation of p_r and synaptic strength.

Materials and Methods

cDNA Constructs. SypH2 was created by isolating the rat synaptophysin cDNA (accession no. NM_012664) from brain total RNA by RT-PCR and ligating into a pEGFP-C1-based expression vector. A cassette containing two copies of superecliptic pHluorin was then inserted into the synaptophysin cDNA between the codons for amino acids 184 and 185 in a PCR approach. tdT-Bsn was generated by replacement of EGFP through tdTomato (36) in the construct EGFP-Bassoon95-3938 (37).

Hippocampal cell cultures, transfections, and immunocytochemistry are described in *SI Materials and Methods*.

Stimulation and Cellular Imaging. Fluorescence microscopy was carried out on a Nikon TE2000 epifluorescence microscope equipped with a 60× (N.A. 1.40) objective, and Smart shutter (Sutter Instrument). Images were acquired at 10 Hz with a Hamamatsu ORCA CCD camera controlled by IPLab software (BioVision). Cultures dishes were mounted in a heated microscope stage platform. Experiments were performed at 35 ± 2 °C in HBS solution containing (in mM) 124 NaCl, 3 KCl, 2 $CaCl_2$, 1 $MgCl_2$, 10 Hepes, and 5 D-glucose adjusted to pH 7.30, supplemented with 10 μM 6,7-dinitroquinoxaline-2,3-dione and 50 μM (2R)-amino-5-phosphonovaleric acid. In the experiments described in Fig. 4, medium was added to the culture after initial measurements and the culture was returned to a CO_2-controlled incubator for 5–6 h before the taking a second set of measurements. Action potentials were elicited by passing 1 ms square current pulses yielding fields of approximately 10 V/cm through platinum electrodes placed 0.5 cm apart. Image acquisition and extracellular stimulation were synchronized using

a Master-8 stimulator (AMPI). Measurements of p_r (100 stimuli at 0.2 Hz), RRP (10 trains of 40 stimuli at 20 Hz) and tdT-Bsn fluorescence were interleaved. After each stimulus train, we waited for 2 min before beginning the next stimulation episode. During the analysis, we confirmed that the stimulus trains did not alter responses to subsequent isolated stimuli.

Image Analysis. Image stacks were background-subtracted and aligned. Maps of stimulus-induced changes in fluorescence intensity were then generated by subtracting an average of three frames taken before stimulation from an average of three frames following stimulation. These maps and tdT-Bsn fluorescence frames were then used to place segments of identical size (36 pixels) on all active zones along an optically identified axon for measurement of responses to train stimulation and isolated stimuli as well as tdT-Bsn fluorescence. tdT-Bsn puncta with more than one discernible fluorescence maximum, likely corresponding to boutons with multiple active zones, were excluded from the analysis. Following fluorescence measurements, traces were corrected for a small amount of photobleaching, amounting to 10–20% for sypH2 throughout the whole experiment. For the direct calculation of p_r, the noise distribution of time averaged responses to isolated stimuli at all synapses of an experiment was determined. Individual stimuli were considered to have resulted in release if the time-averaged sypH2 fluorescence increase (difference of the averaged fluorescence 300 ms prior and subsequent to the stimulus) exceeded a threshold of 1.65 SDs of this noise distribution. This threshold was chosen conservatively to ensure that maximally 5% of stimulation events not eliciting SV exocytosis were falsely counted as release events; however, it may have lead to a slight underestimation of p_r by falsely excluding release events. Unless otherwise noted, error bars depict the SE of responses to 10 stimulus trains (RRP size), 100 isolated low-frequency stimuli (p_r) or 10 measurements of tdT-Bsn fluorescence collected throughout the course of experiments. To determine the significance of changes in measures of RRP and p_r at individual synapses, we performed *t* tests assuming independent samples with unequal variances on time-averaged sypH2 fluorescence increases in response to stimulus trains and low-frequency stimuli.

ACKNOWLEDGMENTS. We thank Drs. Eckart Gundelfinger (Leibniz Institute for Neurobiology, Magdeburg, Germany), Gero Miesenböck (University of Oxford) and Roger Tsien (University of California, San Diego) for generously providing us with the EGFP-Bsn, pHluorin, and tdTomato constructs, respectively. We are grateful to Drs. D. Rasmusson and A. Fine (Dalhousie) for helpful comments. This work was supported by Natural Sciences and Engineering Research Council (Canada) (326821-06) and the Nova Scotia Health Research Foundation (2006-2100). S.K. is a Tier II Canada Research Chair in Molecular Neurobiology of Synaptic Plasticity.

1. Muller KJ, Nicholls JG (1974) Different properties of synapses between a single sensory neurone and two different motor cells in the leech C.N.S. *J Physiol* 238: 357–369.
2. Reyes A, et al. (1998) Target-cell-specific facilitation and depression in neocortical circuits. *Nat Neurosci* 1:279–285.
3. Koester HJ, Johnston D (2005) Target cell-dependent normalization of transmitter release at neocortical synapses. *Science* 308:863–866.
4. Hessler NA, Shirke AM, Malinow R (1993) The probability of transmitter release at a mammalian central synapse. *Nature* 366:569–572.
5. Rosenmund C, Clements JD, Westbrook GL (1993) Nonuniform probability of glutamate release at a hippocampal synapse. *Science* 262:754–757.
6. Huang EP, Stevens CF (1997) Estimating the distribution of synaptic reliabilities. *J Neurophysiol* 78:2870–2880.
7. Dobrunz LE, Stevens CF (1997) Heterogeneity of release probability, facilitation, and depletion at central synapses. *Neuron* 18:995–1008.
8. Zalutsky RA, Nicoll RA (1990) Comparison of two forms of long-term potentiation in single hippocampal neurons. *Science* 248:1619–1624.
9. Zakharenko SS, Zablow L, Siegelbaum SA (2001) Visualization of changes in presynaptic function during long-term synaptic plasticity. *Nat Neurosci* 4:711–717.
10. Emptage NJ, Reid CA, Fine A, Bliss TVP (2003) Optical quantal analysis reveals a presynaptic component of LTP at hippocampal Schaffer-associational synapses. *Neuron* 38:797–804.
11. Enoki R, Hu YL, Hamilton D, Fine A (2009) Expression of long-term plasticity at individual synapses in hippocampus is graded, bidirectional, and mainly presynaptic: Optical quantal analysis. *Neuron* 62:242–253.
12. Sudhof TC (2004) The synaptic vesicle cycle. *Annu Rev Neurosci* 27:509–547.
13. Murthy VN, Schikorski T, Stevens CF, Zhu Y (2001) Inactivity produces increases in neurotransmitter release and synapse size. *Neuron* 32:673–682.
14. Rosenmund C, et al. (2002) Differential control of vesicle priming and short-term plasticity by Munc13 isoforms. *Neuron* 33:411–424.
15. Schoch S, et al. (2002) RIM1alpha forms a protein scaffold for regulating neurotransmitter release at the active zone. *Nature* 415:321–326.
16. Schikorski T, Stevens CF (2001) Morphological correlates of functionally defined synaptic vesicle populations. *Nat Neurosci* 4:391–395.
17. Schikorski T, Stevens CF (1997) Quantitative ultrastructural analysis of hippocampal excitatory synapses. *J Neurosci* 17:5858–5867.
18. Schikorski T, Stevens CF (1999) Quantitative fine-structural analysis of olfactory cortical synapses. *Proc Natl Acad Sci USA* 96:4107–4112.
19. Miesenböck G, De Angelis DA, Rothman JE (1998) Visualizing secretion and synaptic transmission with pH-sensitive green fluorescent proteins. *Nature* 394:192–195.
20. Sankaranarayanan S, De Angelis D, Rothman JE, Ryan TA (2000) The use of pHluorins for optical measurements of presynaptic activity. *Biophys J* 79:2199–2208.
21. Gandhi SP, Stevens CF (2003) Three modes of synaptic vesicular recycling revealed by single-vesicle imaging. *Nature* 423:607–613.
22. Granseth B, Odermatt B, Royle SJ, Lagnado L (2006) Clathrin-mediated endocytosis is the dominant mechanism of vesicle retrieval at hippocampal synapses. *Neuron* 51: 773–786.
23. Zhu Y, Xu J, Heinemann SF (2009) Two pathways of synaptic vesicle retrieval revealed by single-vesicle imaging. *Neuron* 61:397–411.
24. Allen C, Stevens CF (1994) An evaluation of causes for unreliability of synaptic transmission. *Proc Natl Acad Sci USA* 91:10380–10383.
25. Murthy VN, Sejnowski TJ, Stevens CF (1997) Heterogeneous release properties of visualized individual hippocampal synapses. *Neuron* 18:599–612.
26. tom Dieck S, et al. (1998) Bassoon, a novel zinc-finger CAG/glutamine-repeat protein selectively localized at the active zone of presynaptic nerve terminals. *J Cell Biol* 142: 499–509.
27. Krueger SR, Kolar A, Fitzsimonds RM (2003) The presynaptic release apparatus is functional in the absence of dendritic contact and highly mobile within isolated axons. *Neuron* 40:945–957.
28. Harlow ML, Ress D, Stoschek A, Marshall RM, McMahan UJ (2001) The architecture of active zone material at the frog's neuromuscular junction. *Nature* 409:479–484.
29. Phillips GR, et al. (2001) The presynaptic particle web: Ultrastructure, composition, dissolution, and reconstitution. *Neuron* 32:63–77.
30. Takao-Rikitsu E, et al. (2004) Physical and functional interaction of the active zone proteins, CAST, RIM1, and Bassoon, in neurotransmitter release. *J Cell Biol* 164: 301–311.
31. Ryan TA, Ziv NE, Smith SJ (1996) Potentiation of evoked vesicle turnover at individually resolved synaptic boutons. *Neuron* 17:125–134.
32. Bayazitov IT, Richardson RJ, Fricke RG, Zakharenko SS (2007) Slow presynaptic and fast postsynaptic components of compound long-term potentiation. *J Neurosci* 27: 11510–11521.
33. Tsuriel S, et al. (2009) Exchange and redistribution dynamics of the cytoskeleton of the active zone molecule bassoon. *J Neurosci* 29:351–358.
34. De Paola V, et al. (2006) Cell type-specific structural plasticity of axonal branches and boutons in the adult neocortex. *Neuron* 49:861–875.
35. Stettler DD, Yamahachi H, Li W, Denk W, Gilbert CD (2006) Axons and synaptic boutons are highly dynamic in adult visual cortex. *Neuron* 49:877–887.
36. Shaner NC, et al. (2004) Improved monomeric red, orange and yellow fluorescent proteins derived from Discosoma sp. red fluorescent protein. *Nat Biotechnol* 22: 1567–1572.
37. Dresbach T, et al. (2003) Functional regions of the presynaptic cytomatrix protein bassoon: Significance for synaptic targeting and cytomatrix anchoring. *Mol Cell Neurosci* 23:279–291.